Metformin promotes lifespan through mitohormesis via the peroxiredoxin PRDX-2.

Wouter De Haes[1], Lotte Frooninckx[1], Roel Van Assche[1], Arne Smolders[2], Geert Depuydt[1], Johan Billen[3], Bart P. Braeckman[2], Liliane Schoofs[1*], Liesbet Temmerman[1]

[1]Laboratory for Functional Genomics and Proteomics, Department of Biology, KU Leuven, Naamsestraat 59, 3000 Leuven, Belgium [2]Laboratory for Aging Physiology and Molecular Evolution, Department of Biology, Ghent University, Proeftuinstraat 86 N1, 9000 Ghent, Belgium [3]Laboratory of Socioecology and Social Evolution, Department of Biology, KU Leuven, Naamsestraat 59, 3000 Leuven, Belgium

Submitted to Proceedings of the National Academy of Sciences of the United States of America

The anti-glycemic drug metformin, widely prescribed as first-line treatment of type II diabetes mellitus, has lifespan-extending properties. Precisely how this is achieved, remains unclear. Via a quantitative proteomics approach using the model organism *Caenorhabditis elegans*, we gained molecular understanding of the physiological changes elicited by metformin exposure, including changes in branched-chain amino acid catabolism and cuticle maintenance. We show that metformin extends lifespan through the process of mitohormesis and propose a signaling cascade in which metformin-induced production of reactive oxygen species (ROS) increases overall life expectancy. We further address an important issue in aging research, wherein so far, the key molecular link that translates the ROS signal into a pro-longevity cue remained elusive. We show that this beneficial signal of the mitohormetic pathway is propagated by the peroxiredoxin PRDX-2. Because of its evolutionary conservation, peroxiredoxin signaling might underlie a general principle of pro-longevity signaling.

Aging | Metformin | Peroxiredoxin | Proteomics | Reactive oxygen species

Introduction

Metformin, an anti-glycemic biguanide drug and the most common treatment of type II diabetes mellitus, has life-extending capabilities (1, 2). Several other human diseases, such as cancer (3) and nonalcoholic fatty liver disease (4) are also potentially alleviated by metformin treatment. This suggests that metformin acts on common pathways involved in a spectrum of aging-related disorders. Because of its demonstrated beneficial effect on lifespan in the nematode *Caenorhabditis elegans* (5, 6), and in the rodents *Rattus norvegicus* (1) and *Mus musculus* (2), these models facilitate research into the underlying mode of action.

It has been hypothesized that metformin elicits its beneficial effects by mimicking dietary restriction (DR) (7), a regimen wherein a physiological response is triggered by reducing the uptake of nutritive calories. The physiological response to DR causes lifespan extension and delays age-dependent decline from yeast to primates (8). The idea of similarity sprouts from the observed low blood glucose and insulin levels combined with increased glucose utilization in both calorically restricted and metformin-treated animals (7). In addition, metformin-treated worms show phenotypes similar to DR worms (5), and transcript profiles of metformin-treated and DR mice also overlap significantly (9).

Caution is due, however, in referring to DR, because different methods to induce DR in *C. elegans* act through different genes to elicit corresponding effects on lifespan (10–12). Glucose restriction, a specific type of DR, requires the adenosine monophosphate (AMP)-dependent kinase (AMPK) to extend lifespan. Activation of AMPK leads to increased mitochondrial production of reactive oxygen species (ROS), which induces stress defense and results in a net increase in longevity. This process of lifespan extension based on mitochondrial oxidative stress, is known as mitohormesis (13).

Despite its similarities to DR and its widespread use as an anti-glycemic drug, the actual mode of action of metformin is largely unknown and a subject of much debate. In mammals, metformin is generally believed to act through the activation of AMPK, one of the main regulators of cellular energy homeostasis (2, 14–16), but recent research suggests the existence of AMPK-independent mechanisms as well (17, 18). More upstream, metformin is thought to activate AMPK through partial inhibition of complex I of the electron transport chain (ETC) and a resultant increase in the AMP/ATP ratio (19–21), though again, not all data support this theory (16, 22). Important players in metformin-induced lifespan extension in *C. elegans* are the liver kinase B1 ortholog PAR-4, the AMPK ortholog AAK-2 and the SKN-1 transcription factor, which is involved in activating phase II detoxification mechanisms (5). It has recently been demonstrated that in *C. elegans*, metformin partly elicits its effects through altering the folate metabolism of its microbial food source (6), but questions about its direct effects are largely unaddressed. It is for instance unclear how metformin induces AAK-2 and SKN-1 activity. Overall, many gaps remain in our knowledge of metformin-induced lifespan extension.

In order to study the targets of metformin, we performed a proteomic analysis on metformin-treated *C. elegans* and used the results as a framework for follow-up experiments. We observed striking similarities between metformin-treated and glucose-restricted worms and discovered several novel factors involved in mitohormetic regulation of lifespan, including a role for the

Significance

Recently it has been suggested that metformin, the most commonly used anti-diabetic drug, might also possess general health-promoting properties. Elucidating metformin's mode of action will vastly increase its application range, and will contribute to healthy aging. We reveal a signaling cascade in which metformin is able to extend lifespan by increasing the production of reactive oxygen species (ROS). This allowed us to further work at the crossroads of human disease and aging research, identifying a key molecule that is able to translate the ROS signal into a pro-longevity cue: an antioxidant peroxiredoxin is also able to activate a lifespan-promoting signaling cascade, here described in detail. Continued research efforts in this field lead towards a targeted improvement of aging-related complications.

Reserved for Publication Footnotes

Table 1. Functional analysis of differential proteins

Functional analysis of differential proteins	
Pathway enrichment of upregulated proteins[1]	
Pathway	***p*-value**
Valine, leucine and isoleucine degradation	9.85E-09
Citrate cycle (TCA cycle)	1.38E-04
Glycolysis / Gluconeogenesis	2.47E-04
Pyruvate metabolism	4.62E-04
Functional clustering[2]	
Functional clustering of upregulated proteins	
Cluster	**Enrichment score**
Mitochondrial	6.86
Carbohydrate metabolic processes	5.78
Cytoskeleton	4.28
Mitochondrial lumen	4.20
FAD binding and reduction	3.70
Biotin/lipoyl attachment	3.02
Nucleoside binding	3.01
Catabolic processes	2.66
Longevity/aging	2.46
Muscle component	2.39
Catabolism and respiration	2.07
NAD binding and reduction	1.99
Cytoskeleton organization	1.39
Functional clustering of downregulated proteins	
Cluster	**Enrichment score**
Vitellogenins/reproduction	3.20
Mitochondrial	2.68
Galectins	2.07
Longevity/aging	1.59
Biosynthetic processes (DNA/RNA)	1.39

Functional analysis of the differential proteomics data. All enrichment analyses were performed using the Database for Annotation, Visualisation and Integrated Discovery (DAVID) (23). [1]Kyoto Encyclopedia of Genes and Genomes (KEGG) pathways overrepresented ($p < 0.05$) in the group of proteins upregulated after metformin treatment. [2]Functional clustering of proteins, which are significantly altered after metformin treatment. The reported enrichment score was calculated by DAVID based on the Fisher Exact score of each clustered term. The higher the value, the more enriched the cluster. Only clusters with an enrichment score higher than 1 were reported. Complete information can be found in Dataset S1.

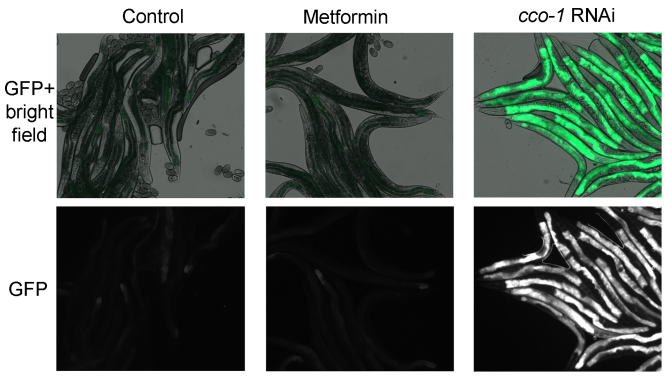

Fig. 1. Metformin treatment does not induce the mitochondria-specific unfolded protein response (UPR^{mt}). Day 1 adult metformin-treated *hsp-6*::GFP worms show no difference in fluorescence when compared to untreated control worms. *hsp-6*::GFP worms were exposed to *cco-1* RNAi as a positive control. *cco-1* encodes a cytochrome c oxidase subunit, an integral part of the mitochondrial electron transport chain (24).

mitochondrial peroxiredoxin PRDX-2, which appears to be responsible for translating oxidative stress into a downstream pro-

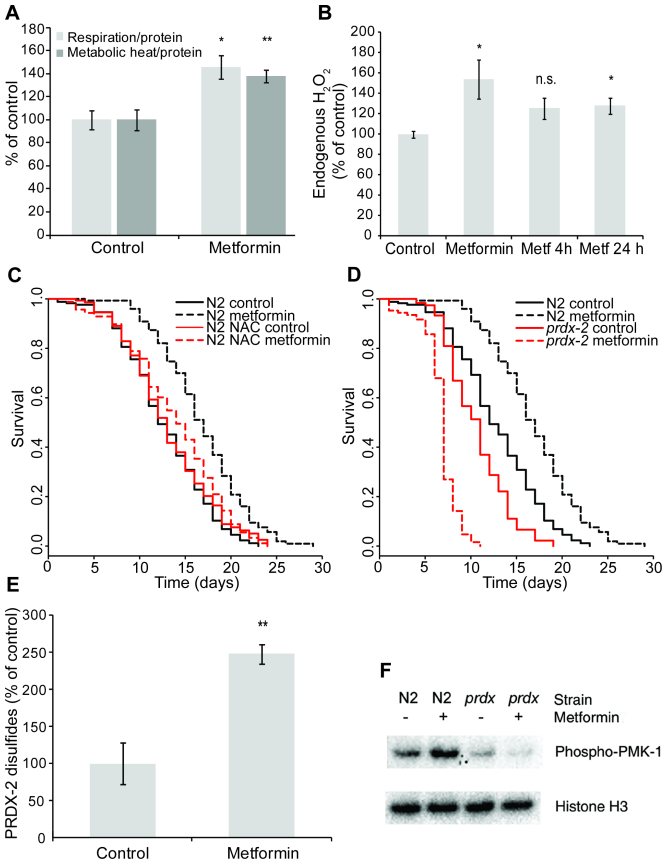

Fig. 2. Metformin increases lifespan according to the principle of mitohormesis, for which it requires PRDX-2. A Metformin treatment increases metabolic heat production ($p < 0.01$**; n = 3 for untreated and n = 4 for treated worms) and respiration ($p < 0.05$*; n = 3). Bars represent mean ± SEM. **B** Metformin induced a significant increase in H_2O_2 release in day 1 adult worms after both continuous exposure during development ($p < 0.05$*; n = 7) and after 24 hours of exposure, starting from the young adult stage ($p < 0.05$*; n = 7 for untreated and n = 5 for treated worms). Exposing the worms for 4 hours before measurement did not result in a significant increase ($p > 0.05^{n.s.}$; n = 7). Bars represent mean ± SEM. **C** The antioxidant N-acetylcysteine (NAC) abolishes the lifespan extending effect of metformin ($p < 0.001$***; n ≥ 169 for each curve, see Table S1). **D** *prdx-2* is required for metformin-induced lifespan extension. Metformin treatment significantly reduces lifespan of *prdx-2* mutants ($p < 0.001$***; n ≥ 127 for each curve, see Table S1). **E** Metformin treatment promotes the formation of PRDX-2 disulfide dimers ($p < 0.01$**), implied to function in signal transduction. Bars represent mean ± SEM (n = 4). **F** PRDX-2 is required for metformin-induced phosphorylation of the p38 MAP kinase PMK-1. Metformin treatment of wild type worms induced phosphorylation of PMK-1, inferred from a larger band observed on the Western blot. This metformin-mediated induction of PMK-1 phosphorylation is absent in *prdx-2* knockout worms. Histone H3 levels were used as a loading control.

longevity signal. In addition to lifespan extension, we also report features that contribute to the healthspan of metformin-treated worms.

Results

Molecular changes in *Caenorhabditis elegans* upon metformin exposure: a proteomic approach

In order to gain a deeper understanding of the physiological changes elicited by metformin exposure, a differential gel-based proteomics experiment was performed. A total of 164 spots with differential abundances were detected, 134 of which could be identified by mass spectrometry. After removal of duplicate iden-

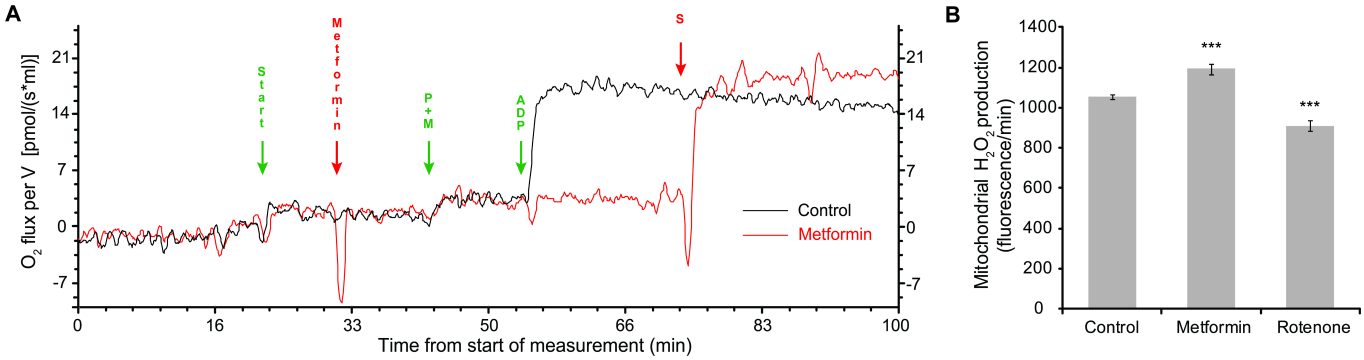

Fig. 3. Metformin inhibits Complex I of the electron transport chain (ETC) in a way distinct from rotenone. A Metformin inhibits complex I but not complex II based respiration. Higher values for O_2 flux indicate higher respiration, negative values indicate a small influx of O_2, usually due to the injection of a compound. The effect of metformin on mitochondrial respiration was measured by sequentially adding compounds to stimulate different parts of the ETC. Green arrows indicate compounds that were added in both the control and metformin-treated cells; red arrows indicate compounds that were only added in the treated cell. After adding an equal volume of mitochondria (↓start), metformin was added to one of the cells (↓metformin). Subsequently, the complex I substrates pyruvate and malate (↓P+M) were added, followed by the addition of ADP (↓ADP), initiating electron transport from complex I. Metformin-treated mitochondria clearly fail to initiate complex I based respiration, thus indicating that metformin inhibits electron transport from complex I *in vitro*. Finally, the complex II substrate succinate (↓S) was added to the metformin-treated cell, which led to a marked increase in mitochondrial respiration, indicating that metformin does not block electron transport from complex II. Two variations of this experiment were executed to also use the potent complex I inhibitor rotenone as a positive control (Fig. S4A) and to add succinate to the negative control condition as well (Fig. S4B). **B** Mitochondria treated with metformin produce H_2O_2 at a higher rate than untreated mitochondria ($p < 0.001$***; n = 3). Treatment with the complex I inhibitor rotenone had the opposite effect ($p < 0.001$***; n = 3).

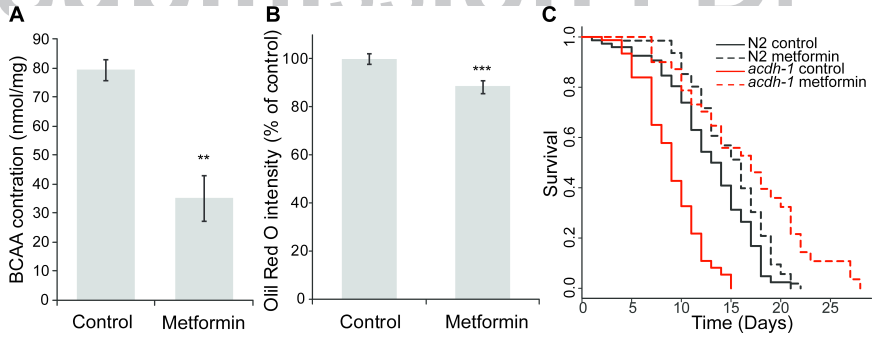

Fig. 4. Metformin induces the branched-chain amino acid (BCAA) degradation and β-oxidation pathways but the β-oxidation enzyme ACDH-1 is not required for metformin-mediated for longevity. A Metformin treatment stimulates the BCAA degradation pathway (Fig. S5) and in turn reduces the concentration of free BCAAs in *C. elegans* ($p < 0.01$**). Bars represent mean ± SEM (n = 6). **B** Metformin-treated worms show reduced fat storage ($p < 0.001$***; n = 30 for untreated and n = 33 for treated worms), possibly indicating increased flux through the β-oxidation pathway. Bars represent mean ± SEM. **C** Deletion of β-oxidation enzyme *acdh-1* results in a proportionally larger effect of metformin on longevity ($p < 0.001$***; n ≥ 54 for each curve, see Table S1) .

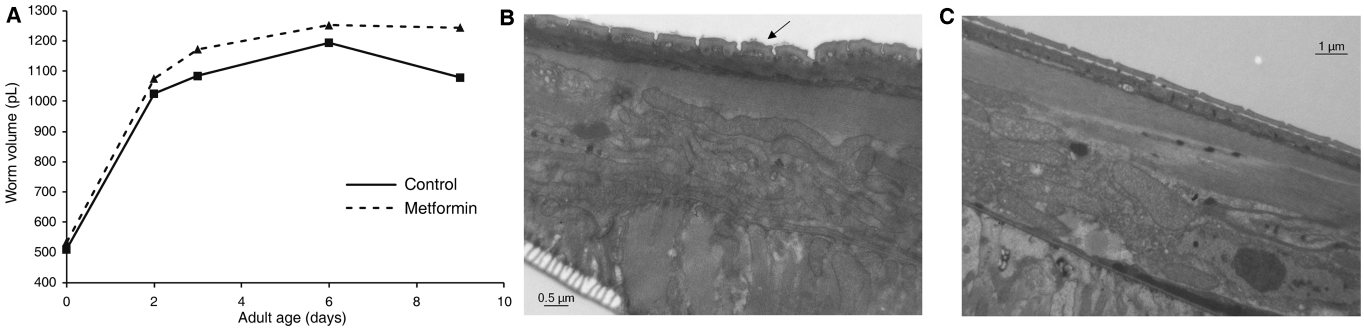

Fig. 5. Metformin attenuates the morphological decline with aging in *C. elegans* **A** Metformin-treated worms retain a stable volume while control worms older than 6 days start shrinking. **B** Electron micrograph of the cuticle of a day 9 adult non-treated wild type worm. Some deformations of the cuticle (seen as "wrinkling", marked with an arrow) are starting to manifest. **C** No structural abnormalities can be seen in a metformin-treated day 9 wild type adult.

tifications, the final analysis resulted in a list of 58 upregulated and 30 downregulated proteins (Dataset S1).

Enrichment analysis (23) of the upregulated proteins resulted in the detection of several overrepresented pathways (Table 1), of which the branched-chain amino acid (BCAA) degradation pathway was most markedly enriched. All other enriched pathways, including glycolysis and the tricarboxylic acid (TCA) cycle, are involved in general energy metabolism. No significant pathway enrichment was observed in the analysis of downregulated proteins. Combined analysis of all differential proteins (both up and down) did not reveal additional pathways of interest.

Further functional clustering was used to subdivide the up- and downregulated proteins into meaningful groups (Table 1). For each functional cluster, detailed information including sub-

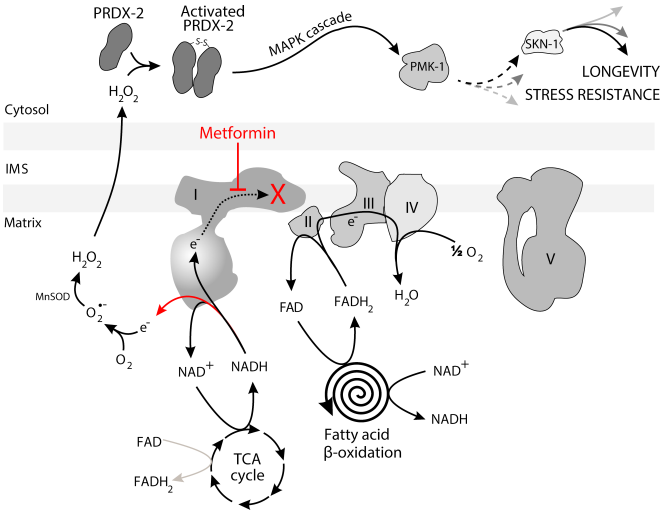

Fig. 6. The mitohormetic signaling cascade as induced by metformin. Metformin induces an increase in activity in several catabolic pathways (Fig. S6), including the TCA cycle and β-oxidation, with β-oxidation producing a relatively higher amount of $FADH_2$ per cycle. This increase in substrate allows for an increase in mitochondrial respiration, which in turn leads to an increase in ROS production, possibly through metformin-mediated perturbation of electron transport (marked in red). These ROS oxidize PRDX-2 peroxiredoxins, which subsequently dimerize and enter their active state. Active PRDX-2 will activate a conserved MAPK cascade containing the p38 MAPK PMK-1, likely leading to the activation of SKN-1 (28) and a concomitant increase in longevity and stress protection (dashed arrows: literature-based evidence; see Fig. S6 for more information on the pathways induced by metformin treatment).

terms and proteins in each group, was gathered to assist in data interpretation (Dataset S1). These results were used as the backbone of hypothesis-driven experiments into the mechanisms induced by metformin treatment.

Metformin does not induce mitochondrial protein unfolding stress

Due to the marked clustering of mitochondrial proteins (Table 1) and metformin's putative inhibitory effect on complex I of the ETC, it needs to be tested whether metformin is capable of inducing the mitochondria-specific unfolded protein response (UPR^{mt}). This is essential because the UPR^{mt} increases lifespan in response to either misfolding of mitochondrial proteins or stoichiometric abnormalities in the ETC complexes (24).

We did not observe upregulation of the UPR^{mt} marker *hsp-6* in worms exposed to metformin (Fig. 1). Additional experiments with higher concentrations of metformin and different exposure times, yielded similar negative results (Fig. S1). As such, lifespan extension of metformin via the induction of the UPR^{mt} is unlikely, which suggests that the drug affects the mitochondria in another way.

Metformin increases lifespan through hormetic phenomena

Metformin has been put forward as a possible DR mimetic (7) and since DR has been linked to mitohormesis (13, 25), we looked into evidence for a role for mitohormesis in metformin-induced lifespan extension. Clustering analysis of the proteomics experiments revealed a significant overrepresentation of several mitochondrial proteins and proteins involved in catabolism (Table 1). These clusters might point to an increase in respiration, one of the hallmarks of mitohormesis (13). Indeed, upon metformin treatment, we observed a significant increase in respiration (45%) and metabolic heat production (38%) (Fig. 2A) in wild type worms. These changes, in combination with the AMPK-dependence of metformin-mediated longevity (5), strongly resemble the mitohormetic pathway (13) and might point toward an increase in ROS production.

To verify whether mitochondrial ROS production was affected by metformin treatment, we measured hydrogen peroxide levels in metformin-treated worms. ROS production was indeed increased (Fig. 2B), further supporting the mitohormesis hypothesis. Induction of ROS production was already clear after 24 hours of exposure to metformin (Fig. 2B). This increase in ROS seems to be an integral part of metformin-induced lifespan extension, as treatment with the potent antioxidants N-acetylcysteine (NAC) (13) and butylated hydroxyanisole (BHA) (26) abolished the positive effect of metformin on lifespan (Fig. 2C and Fig. S2A). Finally, the critical phase for metformin-mediated lifespan extension clearly resembles the critical phase for other mitohormetic stressors (13), as treatment with metformin starting from adulthood onwards or during the first few days of adulthood only, were sufficient to increase lifespan (Fig. S2B). This is opposed to treatment with metformin during larval development only, which had no detectable effect on lifespan (Fig S2B).

Metformin-mediated lifespan extension requires the peroxiredoxin PRDX-2

The mitohormetic pathway as seen during glucose restriction is induced when low availability of glucose causes low energy levels, which in turn activates AMPK (13). AMPK activity increases catabolism and respiration, which results in the increased production of ROS and a resultant activation of hormetic protective mechanisms (13). The largest hiatus in this pathway is the step between the increased ROS production and the induction of stress defense, as no molecule was put forward that might translate the ROS signal into further downstream defense. We therefore set out to reveal this missing link and to further complete the hormetic signaling pathway.

Peroxiredoxins are known hydrogen peroxide scavengers and their oxidized dimeric form is involved in the direct activation of kinases in mammalian cells (27). As the mitochondrial peroxiredoxin PRDX-2 was upregulated during metformin treatment (Dataset S1), this protein is of particular interest as a potential inductor of mitohormesis. Deletion of the *prdx-2* gene results in an extreme decrease in lifespan upon metformin treatment (Fig. 2D). Not only did the positive effect of metformin on lifespan disappear, the *prdx-2* experimental group collapsed when exposed to metformin. Treatment with NAC partially rescued this deleterious effect, implying that excessive ROS production is at least partly responsible for the detrimental effect of metformin on these mutants (Fig. S2C). In support of these results, we observed increased formation of PRDX-2 dimers after metformin treatment (Fig. 3E, Fig. S3). Since these oxidized dimers are likely involved in cellular signaling (27), we propose that PRDX-2 induces pro-longevity signaling during the mitohormetic response to metformin treatment.

One of the potential downstream targets of PRDX-2 is the p38 MAP kinase PMK-1, which is involved in the activation of the SKN-1 transcription factor (28). This transcription factor is in turn required for metformin-mediated longevity (5). Western blot analysis revealed a marked increase in phosphorylation of PMK-1 after metformin treatment. In contrast, deletion of *prdx-2* resulted in an absence of metformin-induced phosphorylation of PMK-1 (Fig. 2F). These data strongly imply that PRDX-2 is required for PMK-1 activation after metformin treatment.

In sum, all these findings subscribe that metformin extends lifespan via mitohormesis in *C. elegans*, and that PRDX-2 is an integral part of the mitohormetic pathway.

Metformin inhibits complex I of the ETC

Metformin is generally believed to act through inhibition of complex I of the ETC (19–21), although some recent findings cast doubt on this (16, 22). Treatment of *C. elegans* with rotenone, another complex I inhibitor, at a concentration that extends longevity, results in a decrease in total oxygen consumption (25). Our finding that metformin increases respiration in worms there-

fore raises the question whether it is truly capable of inhibiting complex I of the ETC.

We tested whether metformin is able to affect electron flow in mitochondria extracted from *C. elegans*, and observed a clear and specific inhibition of electron flow from complex I, while the electron flow from complex II was unaffected (Fig. 3A; Fig. S4A-B). These results, clearly mimicking the inhibitory action of rotenone (Fig. S4A), complement our previous data only if metformin inhibits complex I in a distinct way. To this end, we tested whether metformin and rotenone had different effects on ROS production in mitochondria. At concentrations at which both completely inhibit complex I respiration and after feeding only complex I, metformin increased ROS production while rotenone decreased it (Fig. 3B), implying a fundamental difference between rotenone's and metformin's inhibitory action on complex I.

The BCAA degradation pathway is upregulated during metformin treatment

The BCAAs leucine, isoleucine and valine display a certain duality in relation to health and longevity. On one hand, their effectiveness has been noted in the treatment of liver and cardiac diseases (29, 30) and upregulation of BCAAs is one of the metabolic signatures of the long-lived *daf-2* mutant (31, 32). On the other hand, BCAAs have also been causally linked to the development of insulin resistance, type II diabetes (33) and neuropathologies (34). We set out to confirm the marked upregulation of the BCAA degradation pathway (Table 1; Fig. S5) at the level of free BCAAs in metformin-treated worms. Metformin treatment resulted in a significant decrease (-55%) in the amount of free BCAAs, lending further support to the validity of the proteomics data (Fig. 4A).

Metabolic flux during metformin treatment

One of the most striking properties of metformin as an antidiabetic in humans, is its ability to cause weight loss in patients, through, amongst others, activation of the β-oxidation pathway (2, 35, 36). We observed a 4.3-fold upregulation of the mitochondrial acyl-CoA dehydrogenase family member ACDH-1 after metformin treatment (Dataset S1), defining it as the strongest upregulated protein by a margin. Acyl-CoA dehydrogenases catalyze the first step in the β-oxidation of fatty acids.

We questioned whether the shift in β-oxidation suggested by ACDH-1 induction truly occurs and whether it is involved in metformin-induced lifespan extension. If so, we would grossly expect overall fat levels to drop in treated worms. Measuring fat content in L4 worms, we found evidence for increased β-oxidation as metformin-treated worms showed significantly lower (-11,4%) fat stores (Fig. 4B). A similar reduction in fat content was found in metformin-treated *C. elegans* using different methods (5).

To our surprise, *acdh-1* knockout worms showed an even stronger metformin-induced lifespan extension than wild type worms (Fig. 4C). This implies a more complex interaction between β-oxidation and metformin (see discussion).

Metformin-treated worms attenuate age-related morphological decline.

Aging worms start to show several morphological defects (37) and shrink in size (38) but metformin-treated worms seemed less affected by this phenomenon. After measuring several formalin fixed worms of various ages (Fig. 5A) it became clear that non-treated worms started losing volume after day 6 of adulthood, while metformin-treated worms still retained their normal volume on day 9. Although long-lived mutants are often smaller than their wild type siblings (39), our results fit the recent observations that *within* isogenic populations, the larger animals are generally the longer-lived ones (38).

Muscle and cuticle are known to show severe morphological defects with increasing age in *C. elegans* (37), making them prime targets to question whether these tissues are better maintained in metformin-treated worms. Our proteomics data already pointed to an increase in muscle mass and several changes in the cytoskeleton (Table 1), including upregulation of intermediate filament proteins (Dataset S1). Electron micrographs of 9-day-old control and metformin-treated worms displayed no difference in body wall muscle volume, but there was a clear difference in cuticle morphology (Fig. 5B-C). While the cuticle of 9-day-old adult non-treated worms started showing signs of age-related "wrinkling" and disorganization, the cuticle of metformin-treated worms resembled that of a young animal. Considering the cuticle's known role in maintaining the shape and size of nematodes (40), it can be assumed that it is this amelioration of cuticle deterioration that allows metformin-treated worms to retain a healthy, young morphology.

Discussion

We profiled the effect of metformin in *C. elegans* using a differential proteomics approach and used the resulting data for further examination of its beneficial effects and mode of action.

We observed many changes in the mitochondrial proteome, which might point towards mitonuclear protein imbalance (41) and an altered mitochondrial metabolism. It is therefore probable for metformin to increase lifespan through both the process of mitohormesis and the induction of the UPR^{mt}. However, metformin administration during the larval stages had no effect on lifespan, while the critical phase for UPR^{mt} induction in *C. elegans* is during larval development (24, 42). Because metformin also proved unable to induce the UPR^{mt}, it is not a likely *in vivo* contributor to lifespan extension by metformin in *C. elegans*. Contrary to the UPR^{mt}, the mitohormetic pathway is important for metformin-mediated longevity in this worm.

Hormesis in aging is defined as the process by which a short-term and nonlethal stressor induces the stress response mechanisms of an organism and thereby increases stress resistance and overall life expectancy (43). The mitohormetic pathway, first described in glucose-restricted *C. elegans* (13), states that a low availability of ATP - due to low glycolytic activity - causes activation of AMPK. AMPK in turn promotes general catabolism and mitochondrial respiration, leading to increased production of ROS (the hormetic "stressor"), which subsequently act as messengers to activate further stress defenses, prolonging lifespan. This contradicts the classical oxidative stress theory of aging, which postulates that ROS, due to their ability to damage biomolecules, would be the causative factor of aging (44). We were able to fully reproduce the mitohormetic phenomenon in metformin-treated worms and showed that metformin increases respiration, metabolic heat production and ROS generation in *C. elegans*. Inhibition of ROS signaling abolishes the lifespan-extending effects of metformin, proving that metformin-mediated lifespan extension is dependent on the mitohormetic pathway and most closely resembles the *C. elegans* response to glucose restriction.

Though well studied, some major missing links remained in the mitohormetic pathway, in particular how the ROS signal can be translated to increased lifespan. We were able to demonstrate that the *C. elegans* peroxiredoxin PRDX-2, previously shown to be involved in peroxide and heavy metal resistance (45), is of major importance to this function. Peroxiredoxins are a class of antioxidant proteins characterized by their high susceptibility to cysteine oxidation (46, 47). PRDX-2 is a typical 2-Cys peroxiredoxin (45), of which the active, oxidized form exists as a homodimer (48). It has recently been shown that these dimers are subsequently able to oxidize and activate specific substrates, such as the MAP kinase ASK1 (27), thus resolving how these proteins might be able to translate ROS signals into downstream signaling. In the same vein, our experiments revealed increased formation of PRDX-2 dimers after metformin treatment. These

oxidized dimers might activate ASK1's closest ortholog in *C. elegans,* the MAP kinase NSY-1, which functions upstream in the same signaling pathway as the MAP kinases SEK-1 and PMK-1 (49). This evolutionarily conserved MAP kinase cascade could ultimately activate several downstream targets that mediate stress defense, including SKN-1 (28). We showed that *prdx-2* is required for the downstream activation of PMK-1 in response to metformin exposure, completing the pathway (Fig. 6). Therefore, PRDX-2 may well be the protein responsible for translating oxidative stress into longer lifespan in *C. elegans*. As the longevity-promoting effect of exercise in humans also depends on ROS signaling (50), this pathway may be evolutionary conserved.

AMPK activation is one of the main factors involved in mitohormetic lifespan extension (13, 26). While metformin is known to activate AMPK, exactly how this occurs remains elusive. The most common hypothesis is that metformin is able to partially inhibit complex I of the mitochondrial ETC, which in turn would lead to energy depletion and activation of AMPK (19–21). Recently, this has been debated (16, 22). One of the main arguments against metformin-mediated inhibition of complex I, is the increased activity of pathways that generate energy after metformin treatment. All these pathways require NAD^+ to function, and without efficient recycling of NADH to NAD^+, these pathways are limited in activity. As NADH is mainly recycled at complex I of the ETC, blocking complex I should lead to an increased NADH/NAD^+ ratio and lower catabolism (Fig. 6). As a case in point, the complex I inhibitor rotenone indeed increases the NADH/NAD^+ ratio (51) and lowers the activity of the β-oxidation pathway (16). We were able to show that metformin specifically inhibits complex I of the ETC *in vitro*, albeit in a way that seems fundamentally distinct from rotenone: metformin increased mitochondrial ROS production while rotenone decreased it. High concentrations of rotenone reduce the number of electrons that are transferred from NADH to complex I (high NADH/NAD^+ ratio), hence less electrons can leak out to form ROS. Our results imply that upon metformin treatment, NADH is still able to transfer its electrons, but these are subsequently lost, resulting in increased ROS production (Fig. 6). Based on these data, we suggest that metformin activates AMPK through inhibition of complex I (Fig. S6), which leads to an increase in respiration and a concomitant upregulation of several catabolic pathways - *e.g.* β-oxidation, glycolysis, BCAA catabolism and others - to provide the necessary substrate for the ETC. Likely exacerbated by metformin-mediated perturbation of electron transport, the increase in respiration ultimately leads to a mitohormetic increase in ROS production *in vivo* (Fig. 6). As elevated respiration under physiologically normal conditions often leads to a reduction in ROS production (31), this indeed implies a direct involvement of metformin in the observed increase in ROS.

Treatment of *C. elegans* with metformin results in an overall upregulation of several pathways and processes (including glycolysis and the TCA cycle), most of which are involved in catabolism, supporting the shift towards increased respiration. Two catabolic pathways stood out after metformin treatment: β-oxidation, through the short chain acyl-CoA dehydrogenase ACDH-1, and BCAA degradation. In light of metformin's inhibitory action on complex I but not complex II of the ETC, the observed increase in β-oxidation seems a logical adaptation as it produces a relatively high amount of the complex II substrate $FADH_2$ compared to other catabolic pathways. This might explain why knocking out *acdh-1* adds to the lifespan increase induced by metformin: high activity of the β-oxidation pathway could temporarily increase ATP levels and inactivate AMPK (Fig. 6; Fig. S6). As such, deletion of *acdh-1* could cause a more stringent activation of the mitohormetic pathway. Further experiments will be needed to fully explore the role of β-oxidation in metformin-induced lifespan extension. Our results suggest that the metformin-mediated increase in β-oxidation is likely a compensatory mechanism that is unrelated to metformin-induced longevity.

As for the BCAA degradation pathway, no clear singular correlation between BCAAs and longevity has yet been found in any organism. While some evidence points towards BCAAs as a metabolic signature of long life in *C. elegans* insulin receptor mutants (31, 32), other studies have causally linked BCAAs to the development of insulin resistance, diabetes (33) and neuropathologies (34). Interestingly, BCAAs - leucine in particular - are potent activators of the target of rapamycin (TOR) kinase. Leucine deprivation has previously been associated with reduced TOR signaling (52), which can in turn prolong lifespan and is required for DR-mediated lifespan extension (53). Yet, it remains unclear whether the drop in BCAA levels is necessary for metformin-induced lifespan extension. The reduction in BCAA concentration might result in lower RNA translation into protein, both through inactivation of TOR and a reduction in the amount of substrate necessary for translation (Fig. S6). This in turn may lead to an increase in longevity. There is some precedence for this hypothesis, as amino acid imbalance has been associated with increased longevity in *Drosophila melanogaster* (54), amongst others (55). The recently described bacteria-specific effect of metformin on longevity in *C. elegans* (6) might similarly depend on an amino acid imbalance that occurs through the lowered production of methionine in metformin-treated bacteria (Fig. S6). Our results suggest a hitherto unexplored role for the BCAA degradation pathway in longevity.

Metformin not only increases lifespan, but also healthspan of *C. elegans*: treated worms retain a youthful morphology for a longer time. How metformin is able to attenuate morphological decline of the cuticle in *C. elegans* remains elusive, but the intermediate protein IFC-2 (upregulated after metformin treatment, Dataset S1) seems particularly promising as it is required for normal body shape and cuticle strength (56). Integrity of the cuticle and epidermis might play a more important role in longevity than is generally thought. Deterioration in cuticle structure leads to a loss in barrier function, which may be one of the causes of death of older nematodes (37, 40).

In conclusion, this work reveals new insights in the process of aging, and shows that metformin extends lifespan through mitohormesis. A missing link in the mitohormesis pathway in *C. elegans* has now been assigned: the peroxiredoxin PRDX-2, a protein that translates a ROS signal into a pro-longevity cue. Since peroxiredoxin signaling is evolutionary conserved (27), peroxiredoxins might hold a similar function in humans.

Materials and Methods

C. elegans strains

The following strains were obtained from the *Caenorhabditis Genetics Center* (CGC, University of Minnesota): wild type N2, VC289 *prdx-2(gk169),* VC1011 *acdh-1(ok1489)* and SJ4100 *zcIs13[hsp-6::GFP].* GA507 *glp-4(bn2ts) daf-16(mgDf50)* was provided by the Gems lab. Strains were cultivated on standard nematode growth medium (NGM) seeded with *E. coli* OP50. All strains were outcrossed at least four times, with the exception of SJ4100, which was outcrossed three times. The outcrossed *prdx-2(gk169)* and *acdh-1(ok1489)* strains were renamed LSC555 and LSC556 respectively. All experiments were performed at 20°C unless stated otherwise.

Sampling for 2D-DIGE

The protein samples for 2D-DIGE were taken from *glp-4(bn2ts) daf-16(mgDf50)* worms grown in liquid cultures. The *glp-4(bn2ts)* mutation confers sterility at the permissive temperature of 24°C avoiding contamination with progeny. Preventing germline development also removes abundant contaminating proteins that have no bearing on lifespan, facilitating the analyses. Since *glp-4* mutations cause a slight DAF-16 dependent lifespan increase in *C. elegans* cultured on dead *E. coli* (57), *glp-4(bn2ts) daf-16(mgDf50)* double mutants were used. This does not interfere with the envisaged results, as lifespan extension due to metformin is independent of DAF-16 (5). Cultivating the worms in liquid cultures allowed full control over metformin dosage while ensuring that all worms were fully fed. Additionally, the high-density samples obtained from liquid cultures ensure high protein concentration in 2D-DIGE experiments.

Worms were synchronized by isolating eggs from gravid adults through hypochlorite and NaOH treatments (58) and a subsequent sucrose density centrifugation to separate eggs from dead worms and bacterial debris. L1 worms were added to Fernbach flasks containing S medium (59) and constantly shaken at 24°C. Flash frozen *E. coli* K12 bacteria (Artechno, Isnes, Belgium) were added to the cultures as food source. The concentration of bacteria was checked twice a day and new K12 bacteria were added accordingly to maintain the cultures at optimal food levels (OD_{550} = 1.8). The density of worms in the culture never exceeded 1000 worms/mL to prevent large fluctuations in food availability. When worms reached the L4 stage, cultures were supplemented with 2'-deoxy-5-fluorouridine (FUdR, Sigma-Aldrich) at a final concentration of 100 mg/L. This ensures complete sterility, as *glp-4(bn2ts) daf-16(mgDf50)* worms rarely manage to still produce a few eggs. Once worms reached the adult stage, the test group was exposed to 25 mM of metformin (1,1-dimethylbiguanide hydrochloride, Sigma-Aldrich) for 24 h (see SI Materials and Methods for the determination of the optimal metformin concentration in liquid media; Fig. S7) and protein samples were subsequently taken (see SI Materials and Methods for a complete protocol on protein extraction).

2D-DIGE

Samples were labeled, separated and analyzed as described in Bogaerts *et al.* (60). In short, metformin-treated and non-treated protein extracts were differentially labeled with either Cy3 or Cy5 fluorescent dyes (GE Healthcare). A possible dye bias was taken into account by integrating a dye swap into the experimental design. Differentially labeled samples were pooled, an internal standard labeled with Cy2 was added and the pooled samples were separated in two dimensions. Gels were scanned using an Ettan DIGE Imager (GE Healthcare) and DeCyder 7.0 (GE Healthcare) was used to statistically analyze the images. Spot intensity was compared using a standard Student's t-test with false positive rate correction.

Trypsin digestion and identification of differential proteins

Differential spots were excised using an automated spotpicker (GE Healthcare). The proteins in each spot were digested using a standard in-gel trypsin digestion protocol and subsequently identified using peptide mass fingerprinting (see SI Materials and Methods for a complete protocol).

Clustering of differential proteins

Wormbase gene IDs of differential proteins were uploaded to the bioinformatic tool DAVID (23) to look for enrichment in functional clusters. Functional clustering was performed with high stringency. Pathway enrichment was determined using DAVID by querying the Kyoto Encyclopedia of Genes and Genomes (KEGG).

Lifespan experiments

All lifespan experiments were performed on NGM agar plates or NGM plates supplemented with or without 50 mM of metformin. NAC was used at a concentration of 5 mM and BHA at a concentration of 25 μM, when applicable. For the experiment using BHA, the compound was added from a 1000x concentrated stock in DMSO and an equal volume of DMSO was added to the respective controls. The worms used in the BHA lifespan experiment were pretreated with 25 μM of BHA for one generation before the start of the experiment. For lifespan experiments, twenty L4 stage worms from a synchronous culture were transferred to a plate (either regular NGM or NGM containing one or multiple of the tested compounds), allowed to lay eggs for 24 h and were then removed from the plate. The progeny was transferred to a new plate when they reached the young adult stage and were transferred to new plates during each day of their reproductive period and every 3 days thereafter. Lifespan was monitored every day starting from day 1 of the adult stage: animals that didn't move when gently prodded were marked as dead. Animals that crawled off the plate or died of vulval bursting or internal hatching were censored. Survival curves were statistically analyzed using a Cox Proportional Hazard (to compare the effect of metformin between strains and/or conditions) or LogRank test (to compare a single curve to control; corrected for multiple testing using the Benjamini-Hochberg method). Complete information regarding lifespan experiments can be found in the supplemental data (Table S1).

Measuring *hsp-6*::GFP fluorescence

Synchronized L1 worms of the SJ4100 *zcls13[hsp-6::GFP]* strain were transferred to agar plates containing 0 mM, 50 mM or 100 mM of added metformin. As a positive control, worms were transferred to plates seeded with HT115 *E. coli* containing an RNAi construct targeted against *cco-1* (24). To rule out a specific effect of HT115, plates seeded with HT115 containing an empty vector were used, which caused no fluorescence. Images were acquired using a Zeiss Axio Imager Z1 microscope.

Measuring metabolic heat and respiration

Metabolic activity and respiration measurements were carried out as previously described (61). In short, respiration and metabolic heat production of synchronized day 1 adult worms were measured using a Clark-type electrode respirometer (Strathkelvin, Glasgow, Scotland) and a Thermal Activity Monitor (Thermometric, Järfälla, Sweden) respectively. Treated worms were exposed to 50 mM metformin starting from the L1 stage. Oxygen consumption rates were measured over a span of 15 minutes. After thermal equilibration of the calorimeter, live heat output of each sample was averaged over a 3-hour period. All data were normalized based on the protein concentration in each sample, as this directly correlates to worm biomass. Protein concentrations were determined using a bicinchoninic acid (BCA) kit (Thermo Scientific). Student's t-tests were used to statistically analyze the data.

Quantifying *in vivo* hydrogen peroxide production

Endogenous hydrogen peroxide production was quantified using the Amplex Red hydrogen peroxide kit (Invitrogen, Cat# A22188). Adult worms were washed 3 times with S basal (59), after which the worms were pelleted through centrifugation (800 g, 3 min). From this dense pellet, 50 μl of worms were transferred to a new microcentrifuge tube containing 450 μL of reaction buffer (sodium phosphate buffer supplied with the kit). After centrifugation (800 g, 1.5 min), the reaction buffer was replaced with fresh reaction buffer and 500 μL of Amplex Red working solution (prepared according to the manufacturer's instructions) was added. The worms were allowed to rotate in the dark for one hour, after which they were pelleted through centrifugation (800 g, 1.5 min) and 100 μL of supernatant was transferred to a fluorescence-compatible 96-well plate. Fluorescence (Ex 550 nm, Em 590 nm) was measured and the worm pellet was subjected to protein extraction for normalization. Welch's t-tests with multiple testing correction (Benjamini-Hochberg) were used to statistically analyze the heteroscedastic data.

Measuring mitochondrial respiration

Mitochondria were extracted from worms as previously described (62). Oxygen consumption of the extracted mitochondria was determined using a Clark-type electrode (Oxygraph 2k) and DatLab software (Oroboros instruments, Innsbruck, Austria). An aliquot of 25 μL of mitochondria was incubated in 2mL of air-saturated MiR05 (0.5 mM EGTA, 3 mM $MgCl_2$, 60 mM K-lactobionate, 20 mM taurine, 10 mM KH_2PO_4, 20 mM HEPES, 110 mM sucrose, 1 g/L BSA, pH 7.1) at 20°C. The effect of 25 mM of metformin on electron transport from complex I and complex II was measured as follows: (i) metformin was added from a 1.5 M stock (dissolved in MiR05) until a final concentration of 25 mM was reached (ii) the complex I substrates pyruvate and malate were added from a 1 M stock until a final concentration of 5 mM was reached (iii) ADP was added from a 10 mM stock to initiate complex I respiration (final concentration 25 μM) (iv) when applicable, rotenone was added as positive control at a final concentration of 1 μg/mL from a 400 μg/mL stock (v). To initiate complex II respiration, succinate was added from a 1 M stock until a final concentration of 5 mM was reached.

Measuring mitochondrial hydrogen peroxide production

Mitochondrial hydrogen peroxide production was quantified using a protocol based on the Amplex Red hydrogen peroxide kit (Invitrogen, Cat# A22188). A fluorescence-compatible 96-well plate was prepared and several wells were filled with 96 μL of incubation medium (4 mM ADP, 10 mM pyruvate, 10 mM malate, 10 U Cu/ZnSOD) either containing no additional substance, 25 mM of metformin or 1 μg/mL of rotenone. Subsequently, 100 μL of Amplex Red reaction buffer (100 μM Amplex Red, 4 U/mL horseradish peroxidase dissolved in the sodium phosphate buffer supplied with the kit) was added followed by the addition of 4 μL of freshly extracted mitochondria. The plate was shaken in the dark and every 2 minutes, fluorescence (Ex 550 nm, Em 590 nm) was measured over the span of 1 hour in order to accurately plot the increase in fluorescence over time resulting from hydrogen peroxide production. The resulting curves were statistically analyzed using an ANCOVA analysis.

Anti-PRDX-2 Western blot

A non-reducing anti-PRDX-2 Western blot was performed as described in Oláhová *et al.* (45). In short, synchronized L1 worms were grown on NGM plates with or without 50 mM of added metformin. Proteins were extracted from young adult worms and separated on a non-reducing SDS-PAGE gel. Rabbit anti-PRDX-2 antibodies were kindly provided by Dr Elizabeth Veal. Intensity of PRDX-2 bands was normalized against total protein content of each lane, which was visualized using a Deep Purple (GE Healthcare) total protein stain. A Welch's t-test was performed to analyze the data.

Anti phospho-PMK-1 Western blot

N2 and *prdx-2* worms were synchronized and grown on regular NGM plates. Protein samples of day 1 adult worms were taken as described for the 2D-DIGE experiment. Proteins were separated on an SDS-PAGE gel and rabbit anti-phospho-p38 antibodies were used for visualization (Cell Signaling Technology). Blots were re-incubated with rabbit anti-histone H3 antibodies (Abcam) as a loading control (63).

Measuring fat content through Oil red O staining

Synchronized L1 worms were cultivated on NGM plates with or without 50 mM of added metformin. L4 stage worms were harvested and stained with Oil red O. The staining intensity was acquired for at least 30 worms for each condition (see SI Materials and Methods). A Student's t-test was performed to analyze the data.

Measuring worm volume

Wild type worms were synchronized through hypochlorite treatment and L1 worms were transferred to normal NGM plates or NGM plates supplemented with 50 mM of metformin. FUdR was added to the plates when worms reached the L4 stage at a final concentration of 50 μM. For sampling, worms were washed twice with S basal and subsequently fixed in 4% formaldehyde (3 min at 65°C). Images of the formaldehyde fixed worms were captured and worm width (D) and length (L) were analyzed using a RapidVUE® Particle Shape and Size Analyzer (Beckman Coulter, Pasadena, CA, USA). Worm volume was approximated using the cylinder formula ($V = \pi L(D/2)^2$).

Electron micrographs

Wild type worms were synchronized and sterilized as described for the volume measurements. Worms were harvested when they reached day 9 of adulthood and prepared for electron microscopy (see SI Materials and Methods).

Quantifying concentration of branched-chain amino acids

Wild type worms were synchronized and L4 worms were harvested from the plates. BCAA concentration was measured using a BCAA assay kit (Sigma-Aldrich, Cat# MAK003) according to manufacturer's instructions. Total protein content of the extracts was quantified using the Qubit Protein Assay (Invitrogen) and used for normalization. A Welch's t-test was performed to analyze the data.

Statistical analysis

All statistical analyses, apart from the DeCyder and DAVID analysis, were carried out using R (64). All bar graphs show the mean of biologically independent samples, error bars show SEM. *P*-values < 0.05 were considered significant.

Acknowledgements.

We would like to thank Dr. Elizabeth Veal for providing the anti-PRDX-2 antibodies and Prof. Dr. David Gems for providing the GA507 strain. We would also like to thank Sven Van Bael, An Vandoren, Caroline Vlaeminck and Ineke Dhondt for technical assistance. Several strains were provided by the CGC, which is funded by NIH Office of Research Infrastructure Programs (P40 OD010440). This work was supported by a grant from the Fund for Scientific Research–Flanders (G.04371.0N). LT is an FWO-Flanders postdoc fellow.

1. Anisimov VN et al. (2008) Metformin slows down aging and extends life span of female SHR mice. *Cell Cycle* 7:2769–73.
2. Martin-Montalvo A et al. (2013) Metformin improves healthspan and lifespan in mice. *Nat Commun* 4:2192.
3. Rizos C V, Elisaf MS (2013) Metformin and cancer. *Eur J Pharmacol* 705:96–108.
4. Nakajima K (2012) Multidisciplinary pharmacotherapeutic options for nonalcoholic Fatty liver disease. *Int J Hepatol* 2012:doi:10.1155/2012/950693.
5. Onken B, Driscoll M (2010) Metformin induces a dietary restriction-like state and the oxidative stress response to extend *C. elegans* Healthspan via AMPK, LKB1, and SKN-1. *PLoS One* 5:e8758.
6. Cabreiro F et al. (2013) Metformin Retards Aging in *C. elegans* by Altering Microbial Folate and Methionine Metabolism. *Cell* 153:228–239.
7. Ingram DK et al. (2006) Calorie restriction mimetics: an emerging research field. *Aging Cell* 5:97–108.
8. Fontana L, Partridge L, Longo VD (2010) Extending healthy life span--from yeast to humans. *Science* 328:321–6.
9. Dhahbi JM, Mote PL, Fahy GM, Spindler SR (2005) Identification of potential caloric restriction mimetics by microarray profiling. *Physiol Genomics* 23:343–50.
10. Bishop NA, Guarente L (2007) Two neurons mediate diet-restriction-induced longevity in *C. elegans*. *Nature* 447:545–9.
11. Panowski SH, Wolff S, Aguilaniu H, Durieux J, Dillin A (2007) PHA-4/Foxa mediates diet-restriction-induced longevity of *C. elegans*. *Nature* 447:550–5.
12. Greer EL, Brunet A (2009) Different dietary restriction regimens extend lifespan by both independent and overlapping genetic pathways in *C. elegans*. *Aging Cell* 8:113–27.
13. Schulz TJ et al. (2007) Glucose restriction extends *Caenorhabditis elegans* life span by inducing mitochondrial respiration and increasing oxidative stress. *Cell Metab* 6:280–93.
14. Zhou G et al. (2001) Role of AMP-activated protein kinase in mechanism of metformin action. *J Clin Invest* 108:1167–1174.
15. Stephenne X et al. (2011) Metformin activates AMP-activated protein kinase in primary human hepatocytes by decreasing cellular energy status. *Diabetologia* 54:3101–10.
16. Ouyang J, Parakhia RA, Ochs RS (2011) Metformin activates AMP kinase through inhibition of AMP deaminase. *J Biol Chem* 286:1–11.
17. Foretz M et al. (2010) Metformin inhibits hepatic gluconeogenesis in mice independently of the LKB1 / AMPK pathway via a decrease in hepatic energy state. 120:2355–2369.
18. Ben Sahra I et al. (2011) Metformin, independent of AMPK, induces mTOR inhibition and cell-cycle arrest through REDD1. *Cancer Res* 71:4366–72.
19. Owen MR, Doran E, Halestrap AP (2000) Evidence that metformin exerts its anti-diabetic effects through inhibition of complex 1 of the mitochondrial respiratory chain. *Biochem J* 348:607–614.
20. El-Mir MY et al. (2000) Dimethylbiguanide inhibits cell respiration via an indirect effect targeted on the respiratory chain complex I. *J Biol Chem* 275:223–8.
21. Ota S et al. (2009) Metformin suppresses glucose-6-phosphatase expression by a complex I inhibition and AMPK activation-independent mechanism. *Biochem Biophys Res Commun* 388:311–6.
22. Larsen S et al. (2012) Metformin-treated patients with type 2 diabetes have normal mitochondrial complex I respiration. *Diabetologia* 55:443–9.
23. Huang DW et al. (2007) The DAVID Gene Functional Classification Tool: a novel biological module-centric algorithm to functionally analyze large gene lists. *Genome Biol* 8:R183.
24. Durieux J, Wolff S, Dillin A (2011) The cell-non-autonomous nature of electron transport chain-mediated longevity. *Cell* 144:79–91.
25. Schmeisser S et al. (2013) Neuronal ROS signaling rather than AMPK/sirtuin-mediated energy sensing links dietary restriction to lifespan extension. *Mol Metab* 2:92–102.
26. Zarse K et al. (2012) Impaired insulin/IGF1 signaling extends life span by promoting mitochondrial L-proline catabolism to induce a transient ROS signal. *Cell Metab* 15:451–65.
27. Jarvis RM, Hughes SM, Ledgerwood EC (2012) Peroxiredoxin 1 functions as a signal peroxidase to receive, transduce, and transmit peroxide signals in mammalian cells. *Free Radic Biol Med* 53:1522–30.
28. Inoue H et al. (2005) The *C. elegans* p38 MAPK pathway regulates nuclear localization of the transcription factor SKN-1 in oxidative stress response. *Genes Dev* 19:2278–83.
29. Lam VW, Poon RT (2008) Role of branched-chain amino acids in management of cirrhosis and hepatocellular carcinoma. *Hepatol Res* 38:S107–15.
30. Mitręga K et al. (2011) Beneficial effects of l-leucine and l-valine on arrhythmias, hemodynamics and myocardial morphology in rats. *Pharmacol Res* 64:218–25.
31. Fuchs S et al. (2010) A metabolic signature of long life in *Caenorhabditis elegans*. *BMC Biol* 8:14.
32. Depuydt G et al. (2013) Reduced insulin/insulin-like growth factor-1 signaling and dietary restriction inhibit translation but preserve muscle mass in *Caenorhabditis elegans*. *Mol Cell Proteomics* 12:3624–39.
33. Newgard CB (2012) Interplay between lipids and branched-chain amino acids in development of insulin resistance. *Cell Metab* 15:606–14.
34. De Simone R et al. (2013) Branched-chain amino acids influence the immune properties of microglial cells and their responsiveness to pro-inflammatory signals. *Biochim Biophys Acta* 1832:650–9.
35. Stachowicz A et al. (2012) Proteomic analysis of liver mitochondria of apolipoprotein E knockout mice treated with metformin. *J Proteomics* 77:167–175.
36. Lee A, Morley JE (1998) Metformin decreases food consumption and induces weight loss in subjects with obesity with type II non-insulin-dependent diabetes. *Obes Res* 6:47–53.
37. Herndon LA et al. (2002) Stochastic and genetic factors influence tissue-specific decline in ageing C. elegans. *Nature* 419:808–14.
38. Pincus Z, Smith-Vikos T, Slack FJ (2011) MicroRNA predictors of longevity in Caenorhabditis elegans. *PLoS Genet* 7:e1002306.
39. Iser WB, Wolkow CA (2007) DAF-2/insulin-like signaling in C. elegans modifies effects of dietary restriction and nutrient stress on aging, stress and growth. *PLoS One* 2:e1240.
40. Chisholm AD, Xu S (2012) The Caenorhabditis elegans epidermis as a model skin. II: differentiation and physiological roles. *Wiley Interdiscip Rev Dev Biol* 1:879–902.
41. Houtkooper RH et al. (2013) Mitonuclear protein imbalance as a conserved longevity mechanism. *Nature* 497:451–7.
42. Dillin A et al. (2002) Rates of behavior and aging specified by mitochondrial function during development. *Science* 298:2398–401.
43. Rattan SIS (2008) Hormesis in aging. *Ageing Res Rev* 7:63–78.
44. Harman D (1956) Aging—a theory based on free-radical and radiation-chemistry. *J Gerontol* 11:298–300.
45. Oláhová M et al. (2008) A redox-sensitive peroxiredoxin that is important for longevity has tissue- and stress-specific roles in stress resistance. *Proc Natl Acad Sci U S A* 105:19839–19844.
46. Yang K-S et al. (2002) Inactivation of human peroxiredoxin I during catalysis as the result of the oxidation of the catalytic site cysteine to cysteine-sulfinic acid. *J Biol Chem* 277:38029–36.
47. Thamsen M, Kumsta C, Li F, Jakob U (2011) Is Overoxidation of Peroxiredoxin Physiologically Significant? *Antioxid Redox Signal* 14:725–730.
48. Hall A, Karplus PA, Poole LB (2009) Typical 2-Cys Peroxiredoxins: Structures, mechanisms and functions. *FEBS J* 276:2469–2477.
49. Kim DH et al. (2002) A conserved p38 MAP kinase pathway in *Caenorhabditis elegans* innate immunity. *Science* 297:623–6.
50. Ristow M et al. (2009) Antioxidants prevent health-promoting effects of physical exercise in humans. *Proc Natl Acad Sci U S A* 106:8665–8670.
51. He Q, Wang M, Petucci C, Gardell SJ, Han X (2013) Rotenone induces reductive stress and triacylglycerol deposition in C2C12 cells. *Int J Biochem Cell Biol* 45:2749–55.
52. Xiao F et al. (2011) Leucine deprivation increases hepatic insulin sensitivity via GCN2/mTOR/S6K1 and AMPK pathways. *Diabetes* 60:746–56.
53. Hansen M et al. (2007) Lifespan extension by conditions that inhibit translation in *Caenorhabditis elegans*. *Aging Cell* 6:95–110.
54. Grandison RC, Piper MDW, Partridge L (2009) Amino acid imbalance explains extension of lifespan by dietary restriction in *Drosophila*. *Nature* 462:1061–1064.
55. Miller RA et al. (2005) Methionine-deficient diet extends mouse lifespan, slows immune and lens aging, alters glucose, T4, IGF-I and insulin levels, and increases hepatocyte MIF levels and stress resistance. *Aging Cell* 4:119–25.
56. Karabinos A, Schmidt H, Harborth J, Schnabel R, Weber K (2001) Essential roles for four cytoplasmic intermediate filament proteins in *Caenorhabditis elegans* development. *Proc Natl Acad Sci U S A* 98:7863–8.
57. McElwee JJ, Schuster E, Blanc E, Thomas JH, Gems D (2004) Shared transcriptional signature in *Caenorhabditis elegans* Dauer larvae and long-lived daf-2 mutants implicates detoxification system in longevity assurance. *J Biol Chem* 279:44533–43.
58. Wood WB (1988) *The nematode Caenorhabditis elegans* (Cold Spring Harbor Laboratory Press, New York, NY).
59. Stiernagle T (2006) in *WormBook, ed. The C. elegans Research Community, WormBook*, pp doi/10.1895/wormbook.1.101.1, http://www.wormbook.
60. Bogaerts A, Beets I, Temmerman L, Schoofs L, Verleyen P (2010) Proteome changes of *Caenorhabditis elegans* upon a *Staphylococcus aureus* infection. *Biol Direct* 5:11.
61. Braeckman BP, Houthoofd K, De Vreese A, Vanfleteren JR (2002) Assaying metabolic activity in ageing *Caenorhabditis elegans*. *Mech Ageing Dev* 123:105–19.
62. Brys K, Castelein N, Matthijssens F, Vanfleteren JR, Braeckman BP (2010) Disruption of insulin signalling preserves bioenergetic competence of mitochondria in ageing *Caenorhabditis elegans*. *BMC Biol* 8:91.
63. Wirth M et al. (2009) HIS-24 linker histone and SIR-2.1 deacetylase induce H3K27me3 in the *Caenorhabditis elegans* germ line. *Mol Cell Biol* 29:3700–9.
64. R Core Team (2013) R: A language and environment for statistical computing. R Foundation for Statistical Computing, Vienna, Austria. Available at: http://www.r-project.org/.